IEEE Access
Multidisciplinary | Rapid Review | Open Access Journal

Received May 26, 2021, accepted June 10, 2021, date of publication June 14, 2021, date of current version June 24, 2021.

*Digital Object Identifier 10.1109/ACCESS.2021.3089367*

# Temporal and Spatial Distribution of Suspended Sediment Concentration in Lakes Based on Satellite Remote Sensing and Internet of Things

**MING ZENG[1], JUN PENG[2], LING JIANG[2], AND JINGJUAN FENG[2]**
[1]Jiangxi Yangtze River Economic Zone Research Institute, Jiujiang University, Jiujiang 332005, China
[2]School of Geographic Information and Tourism, Chuzhou University, Chuzhou 239000, China

Corresponding author: Jun Peng (ru5293@163.com)

This work was supported in part by the Natural Science Research Project in colleges and universities of Anhui province under Contract KJ2020A0719, in part by the Key Project of Research and Development in Chuzhou Science and Technology Program under Contract 2020ZG016, and in part by the Scientific Research Foundation of Chuzhou University under Contract 2020qd02.

**ABSTRACT** The measurement of the concentration of suspended sediment in a water body is a very important content in the observation of hydrological elements, and it is also one of the important parameters for calculating the sediment resuspension flux. In order to accurately predict the distribution of lake sediment, this paper uses satellite remote sensing data to invert the suspended sediment concentration. The key to the quantitative inversion is the atmospheric correction and the suspended sediment concentration inversion algorithm. In this paper, satellite remote sensing technology and Internet of Things technology are combined to establish a new type of lake suspended sediment concentration distribution model. First of all, this paper combines the results of satellite remote sensing inversion and the results of on-site water sample inspections of the Internet of Things to obtain the original hydrological data of suspended sediment in the lake. Secondly, this paper combines ADAM with deep learning technology to simulate the lake flow field and predict the dynamic process of suspended sediment pollution under different conditions. Finally, through experimental simulation and field sampling experiments, the validity of the lake suspended sediment concentration model established in this paper is verified. This model can provide assistance for relevant agencies to grasp the temporal and spatial distribution of suspended sediment concentration in regional lakes in a comprehensive and timely manner, and can obtain the overall characteristics of the study area and the impact of humanistic engineering construction.

**INDEX TERMS** Lake sediment concentration, Internet of Things, temporal and spatial distribution, satellite remote sensing, ADAM.

## I. INTRODUCTION

The concentration of suspended sediment in a water body determines the transparency, turbidity and water color of the water body and other optical properties. The distribution pattern of suspended sediment is of great significance to the study of water quality, landform, ecological environment, coastal engineering, port construction, etc. [1], [2]. With the help of remote sensing technology, the information on the concentration of suspended sediment that traditional methods require a lot of work can be obtained faster, better, and more easily. Water color remote sensing is based on the spectral characteristics of water absorption and scattering in visible light or near-infrared, using the water spectral radiation data measured by aviation and aerospace sensors to interpret the relevant phenomena and parameters of the water body [3].

In recent years, the application of remote sensing inversion of suspended sediment has been more refined. With the help of remote sensing technology, the information on the concentration of suspended sediment that traditional methods require a lot of work can be obtained faster, better and easier [4]. Water color is an important factor that characterizes the water environment. It is related to the physical properties, chemical composition, and dynamic state of the water, especially the suspended sediment, phytoplankton, and yellow substances in the sea [5], [6]. Fettle *et al.* used Sealifts

The associate editor coordinating the review of this manuscript and approving it for publication was Yuan Tian.

images to estimate the transmission of suspended particulate matter in the southern part of the North Sea. Field tests and numerical simulation results showed that the sediment concentration data measured by satellites is generally lower than the field test data [7]. Through satellite remote sensing, we can grasp the spatial distribution status of suspended sediment, and discuss the transportation law and sedimentary characteristics of sediment in a complex environment. T Haryanto *et al.* used ASTER, ALOS, SPOT-4 satellite data to monitor changes in Barron's estuary environment. They showed that a large amount of silt thrown into the river led to the settlement of the estuary and the coastal zone, which caused an impact on the ecological environment of the estuary and coastal zone. Certain influence [8]. The concentration of suspended sediment in the water body is a key parameter for analyzing changes in erosion and deposition on the coast of an estuary and estimating the flux of materials from rivers into the sea [9]. Cai *et al.* used remote sensing technology to conclude that coastal projects such as large bridges will affect the transport and resuspension of suspended sediment, and have a certain impact on the distribution of suspended sediment [10].

Through analysis, we find that the above results are mostly analyzed by engineering cases, and the results only involve a certain static problem of the specific project. In terms of suspended sediment, there is still a lack of research on the changes in hydrodynamics and pollution diffusion over time, and whether the predicted results are consistent with the actual situation is also lack of investigation and verification, so in-depth research is needed [11]. After comparing the historical data of Landsat8 OLI and MODIS data, Barnes *et al.* analyzed the impact of the project to widen the Miami port and concluded that the turbidity current caused by the dredging project had an adverse impact on the ecological environment of the coral communities near the Miami port [12]. Under the current limitations of sensor technology, taking into account the technical cost and technological level, it will take a long period of time to improve the sensor. However, the current data is difficult to meet the needs of many applications. In order to improve the accuracy of remote sensing data, experts and scholars in various applications have carried out a series of scale reduction research work [13]. In this regard, its fundamental purpose is to enhance the temporal and spatial resolution of remote sensing data, so that remote sensing data has high temporal resolution at the same time.

The main purpose of this thesis is to use the concentration of suspended sediment as the research object to explore the method of remote sensing to monitor the water quality of large lakes. The general task of the research is to establish a high-precision model to invert the suspended sediment concentration from GOCI satellite images, and then perform simple spatial dynamics and day-night cycle analysis of the sediment [14]. This paper combines the results of satellite remote sensing inversion and the results of on-site water sample inspections of the Internet of Things to obtain the original hydrological data of suspended sediment in lakes. Secondly, this paper combines ADAM and deep learning technology to simulate the lake flow field to predict the dynamic process of suspended sediment pollution under different conditions. The second part of this article introduces related research on the Internet of Things and the concentration of suspended sediment in lakes, and the third part discusses the research on satellite data inversion and the architecture of the Internet of Things, as well as the simulation of suspended sediment concentration in lakes based on ADAM and deep learning. The fourth part carried out the simulation analysis and testing process for the aforementioned model. Finally, the fifth part of this article discusses the research conclusions and shortcomings, and prospects for future research.

The research contributions of this article are as follows:

(1) This article combines satellite remote sensing technology and Internet of Things technology to establish a new type of lake suspended sediment concentration distribution model.

(2) This paper combines the results of satellite remote sensing inversion and the results of on-site water sample inspections of the Internet of Things, thereby obtaining the original hydrological data of suspended sediment in the lake.

(3) This paper combines ADAM with deep learning technology to simulate the lake flow field and predict the dynamic process of suspended sediment pollution under different conditions.

(4) The validity of the lake suspended sediment concentration model established in this paper is verified through experimental simulation and field sampling test.

The writing organization of the thesis is as follows:

The second section discusses related work, the third section discusses the research methods of the paper, the fourth section carries on the simulation experiment, and the fifth section summarizes the full text.

## II. RELATED WORK

### A. INTERNET OF THINGS TECHNOLOGY

The Internet of Things (IoT) can be regarded as a far-reaching vision with technical and social significance [15]. From the perspective of technology standardization, IoT can be regarded as the infrastructure of the global information society, providing physical interconnection (physical and virtual) on the basis of existing and emerging interoperable information and communication technologies (ICT) Advanced business [16]. Through identification, data capture, processing, and communication capabilities, IoT can make full use of ''things'' to provide services for various applications, while ensuring security and privacy requirements.

There are three key technologies in IoT systems: RFID, sensors and embedded systems. Sensor technology is the foundation of the Internet of Things. The Internet of Things terminal realizes the communication between things and the external network through sensors. The sensor can convert the analog signal sensed by the Internet of Things terminal into a digital signal for easy transmission. It is the Internet

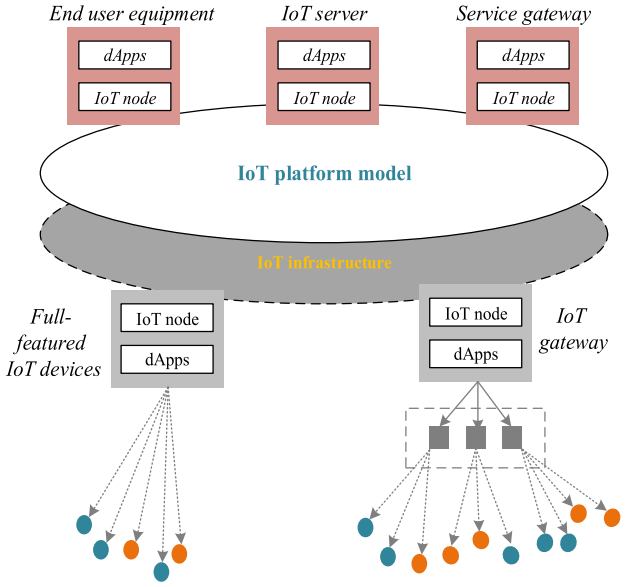


**FIGURE 1.** Schematic diagram of IoT business platform model.

of Things. Intermediary with external networks [17]. The application of RFID technology in the Internet of Things can speed up the identification and increase the operating speed of the Internet of Things. Embedded systems can integrate some specific functions into IoT terminals, making it easier for developers to develop IoT devices that meet the needs of different industries. Compared with traditional IoT products, full-featured IoT devices must have electronic components such as networking, computing, and storage for participating in blockchain consensus and storage, which will inevitably increase the volume and cost of the product [18].

### B. LAKE SUSPENDED SEDIMENT CONCENTRATION

The distribution, diffusion, and settlement of suspended sediment in water bodies affect ports, navigation channels, and ecological environment. Therefore, the measurement of its content is a very critical issue for the study of estuary marine sedimentation dynamics and nearshore engineering. Suspended sediment, chlorophyll and yellow substances have obvious spectral characteristics in water bodies, which can be regarded as direct water quality parameters [19]. Substances such as total nitrogen and total phosphorus have no obvious spectral characteristics, but are inherently related to direct water quality parameters as indirect water quality parameters. The essence of remote sensing application is inversion. Suspended sediment has obvious spectral characteristics and can be monitored on a large scale by inversion methods [20], [21].

The content of suspended sediment in seawater is one of the important parameters for calculating sediment resuspension flux. According to the resuspension flux, the intrusion and siltation status of the seabed or tidal flat in a certain area can be understood [22]. On the one hand, domestic and foreign countries are striving to develop technologies for measuring suspended sediment using optical, acoustic, and other physical methods. On the other hand, they have begun to combine suspended sediment measuring instruments and ocean dynamic element measuring instruments into a system, which has a strong impact on the characteristics of suspended sediment and A comprehensive study of the marine dynamic conditions that caused its migration [23]. Since remote sensing technology has been applied to ocean water color research, many researchers have focused on atmospheric correction of remote sensing data.

## III. THE PROPOSED SCHEME

In the second part of this article, we introduced related research on the Internet of Things and the concentration of suspended sediment in lakes. Next, in the third part of this article, we will describe the structural design of the Internet of Things for monitoring the concentration of suspended sediment in lakes. In addition, we will also discuss the inversion of lake suspended sediment concentration based on ADAM and deep learning satellite data.

### A. IOT STRUCTURE DESIGN

Both the user side and the service side need to participate in the IOT system with certain Internet of Things entities. The Internet of Things entities on the user side are mostly "end-user devices", such as smart phones, and may also be "full-featured Internet of Things devices" or "Internet of Things devices with limited capabilities" [10]. The structural design analysis of the Internet of Things is the core of the IOT product design model. On the one hand, the process of structural design is the process of clarification and optimization of the product business process, so as to save product development and production costs and provide consumers with a better user experience [24]. The overall task of the research is to establish a high-precision model to retrieve the suspended sediment concentration from GOCI satellite images, and then perform simple spatial dynamics and day-night cycle analysis of the sediment. This paper combines the results of satellite remote sensing inversion and the results of on-site water

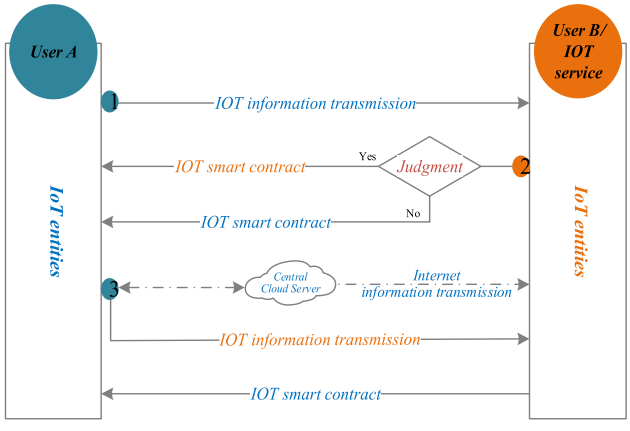


**FIGURE 2.** Interaction flow chart of IoT architecture.

sample inspections of the Internet of Things to obtain the original hydrological data of suspended sediment in lakes.

The server is generally an IoT service company or organization. Generally speaking, the Internet of Things entity on the server side is generally an ''Internet of Things server'' or ''traditional Internet of Things application or service''. On the other hand, structural design is a bridge between designers' creative ideas and programming technicians [25]. The visualized interactive flowchart presented by the designer can explain the specific logic of the product business more clearly, and promote the accurate and efficient completion of product technology. Of course, it may also be the same IoT entity device as the user end. It may also be other ordinary users [26].

### B. INVERSION OF SUSPENDED SEDIMENT CONCENTRATION SATELLITE DATA BASED ON ADAM AND DEEP LEARNING

The earliest atmospheric correction algorithm is only applicable to non-turbid water bodies. Gordon was the first researcher to perform atmospheric correction on ocean water color images. He pioneered an atmospheric correction algorithm based on CZCS data. In addition, many researchers use the ultraviolet band (UV) for atmospheric correction [27], [28]. Because debris and yellow organic matter have a strong absorption effect in the ultraviolet band, even in a high-concentration suspended sedimentation environment, compared with the visible light band or even the near-infrared band, the reflection rate from water at the ultraviolet band is very small, can be regarded as zero.

After atmospheric correction, the out-of-water reflectivity can be obtained. The reflectivity from water needs to be linked to the optical properties of the water body to invert the concentration of suspended sediment. There are many scholars devoted to this research [29]. This process involves two models: forward and inversion. Forward modeling refers to the process of knowing the concentration of various components in the water body and calculating the reflectivity from water [30], [31].

In order to achieve the inversion of suspended sediment concentration satellite data, we introduced ADAM and deep learning algorithms in the process [32]. Each network weight (parameter) maintains a learning rate, and is adjusted individually as learning expands. This method calculates the adaptive learning rate of different parameters from the budget of the first and second moments of the gradient [33]. Among them, deep belief networks, self-encoding networks and generative adversarial networks are all generative models, which are mainly used in the field of unsupervised learning, while recurrent neural networks mainly deal with the learning problem of serialized data, and convolutional neural networks are mainly used in the field of unsupervised learning. Supervise the field of learning. Among them, convolutional neural network technology is the main research tool of this article.

Correlation is used to describe the relationship between two signals, divided into cross-correlation and auto-correlation. Correlation in target tracking based on correlation filtering refers to cross-correlation.

$$E = E\left(y_1^l, \ldots, y_n^l\right) = \sum_j^h \left(y_j^l - t_j\right) \tag{1}$$

$$w_{im}^{l-1} = w_{im}^{l-1} - \eta \times \frac{\partial E}{\partial w_{im}^{l-1}} \tag{2}$$

The Adam optimization algorithm is an extension of the stochastic gradient descent method, and has recently been widely used in deep learning applications in computer vision and natural language processing. Adam is different from the classic stochastic gradient descent method [34].

$$f1(x) = \frac{1}{1 + e^{-\lambda x}} \tag{3}$$

$$\Delta w_{ij} = \eta \delta_j x_{ij} \tag{4}$$

Deep learning is gradually improved and developed on the basis of artificial neural networks.

$$E = \sum_{j=1}^{k} \sum_{x_i \in C_j} D^2(i, j) \tag{5}$$

Stochastic gradient descent maintains a single learning rate (called alpha) for all weight updates, and the learning rate does not change during the training process.

$$U_m = \sum_t W_{mt} I_t + \theta_m \tag{6}$$

$$H_m = f(U_m) \tag{7}$$

The actual measured suspended sediment data is interpolated, and the obtained surface suspended sediment concentration contour map is compared with the suspended sediment surface concentration distribution map calculated by remote sensing.

$$\delta_k = o_k'(t_k - o_k) = o_k(1 - o_k)(t_k - o_k) \tag{8}$$

Deep learning models mainly include deep belief networks, self-encoding networks, generative adversarial networks, recurrent neural networks and convolutional neural networks.

$$g(x, y) = \exp\left(-\frac{x^2 + \gamma^2 y^2}{2\sigma^2}\right)\left(2\pi \frac{x}{\lambda} + \psi\right) \tag{9}$$

Therefore, the correlation filter can be calculated using the following formula:

$$T(i) = T_0(1 - i)^n + \binom{n}{1} T_1(1 - i)^{n-1} t + \cdots + T_n i^n, i \in [0, 1] \tag{10}$$

In order to reduce the number of parameters in the model, a factorization convolution method is proposed in ECO. The filter power learned in C-COT contains negligible energy, which is especially obvious for high-dimensional depth features.

$$\delta_k = o_k' \sum_{k \in outputs} w_{kh}\delta_k = o_k(1 - o_k) \sum_{k \in outputs} w_{kh}\delta_k \tag{11}$$

$$\delta_n = (O_n - T_n) O_n (1 - O_n) \tag{12}$$

Each box represents a filter, and the depth of the color represents the effect of the filter.

$$\sigma_m = \sum_n \delta_n V_{nm} H_m (1 - H_m) \tag{13}$$

The remote sensing base map shows the area with high albedo, that is, the area with high concentration of suspended sediment on the surface.

$$\begin{cases} \ddot{\varphi}_a = -(b_1 + \Delta b_1)\dot{\varphi}_a - (b_2 + \Delta b_2)\varphi_a \\ -(b_3 + \Delta b_3)\delta_\varphi + fd_1 \\ \ddot{\psi}_a = -(b_1 + \Delta b_1)\dot{\psi}_a - (b_2 + \Delta b_2)\psi_a \\ -(b_3 + \Delta b_3)\delta_\psi + fd_2 \\ \ddot{\gamma} = -(d_3 + \Delta d_3)\delta_\gamma + fd_3 \end{cases} \tag{14}$$

$$\gamma\,(x_i, S_t) : |\{i\,|a_i\,(t) \geq x_i\}| \tag{15}$$

The k- $\varepsilon$ two-equation turbulence model is constructed, and it can be further obtained:

$$M_n \ddot{\varphi}_a + h_n(\varphi_a, \dot{\varphi}_a) = u(t) + \rho(t) \tag{16}$$

$$\rho(t) = -\Delta M \ddot{\varphi}_a - \Delta h(\varphi_a, \dot{\varphi}_a) + d(t) \tag{17}$$

In the remaining areas, the remote sensing base map shows areas with low albedo, that is, areas with low concentrations of suspended sediment on the surface.

$$f(x) = E^n[f_1(x), f_2(x), \ldots, f_p(x)]^T \tag{18}$$

However, the concentration contours of surface suspended matter are sparsely distributed, and the gradient changes are not obvious.

$$\min_{x \in R} f(x) R = \{X \in E^n | g_i(x) = 0, h_j(x) = 0\} \tag{19}$$

$$x = [x_1 x_2, \ldots, x_n]^T, \quad y = [y_1 y_2, \ldots, y_n]^T \in E^n \tag{20}$$

After atmospheric correction, the reflectivity outside water can be obtained. The reflectivity from the water needs to be correlated with the optical properties of the water body to reverse the concentration of suspended sediments. There are many scholars dedicated to this research.

This process involves two models: forward and reverse. Forward modeling refers to the process of knowing the concentration of various components in the water body and calculating the reflectivity of the water. As shown in Table 1 and Figure 4, we collate the measured sea surface temperature data with the remotely sensed sea surface temperature data calculated at the corresponding point on the day, as shown in Table 1 and Figure 4. Table 1 lists satellite remote sensing sea surface temperature data. Figure 4 depicts the trend of sea surface temperature data from satellite remote sensing.

It can be seen from Figure 3 that the inversion data has a good correlation with the measured data, and the distribution of sea surface temperature can be quantitatively explained within the error range. On the whole, the accuracy meets the requirements. Due to the large amount of calculation of the convolution operation, the nature of the fast Fourier transform is used to transform the convolution operation in the space domain into the multiplication operation in the frequency domain, which can greatly improve the operation speed.

**TABLE 1. Satellite remote sensing of sea surface temperature data.**

| Dimension(º N) | longitude(º N) | Measured SST(ºC) | Inversion SST(ºC) | ▲T(ºC) |
|---|---|---|---|---|
| 34.00062 | 123.5856 | 27.873 | 27.39383 | -0.479171 |
| 34.00055 | 123.9992 | 27.988 | 27.79321 | -0.194787 |
| 37.89 | 123.0638 | 26.102 | 25.65576 | -0.446238 |
| 38.07695 | 123.1878 | 25.573 | 25.90704 | 0.334043 |
| 36.46447 | 122.9906 | 25.022 | 24.67184 | -0.350156 |
| 37.7125 | 122.9133 | 25.95 | 25.96686 | 0.016858 |
| 38.10078 | 121.4673 | 24.03 | 24.456 | 0.426 |
| 37.8009 | 121.4677 | 24.494 | 24.92477 | 0.430774 |
| 37.91985 | 120.9671 | 23.907 | 23.7811 | -0.125903 |
| 39.30638 | 119.7051 | 21.761 | 21.49463 | -0.266371 |
| 37.7089 | 121.4836 | 24.299 | 25.0398 | 0.740795 |
| 33.49667 | 123.9973 | 27.521 | 27.88873 | 0.367733 |
| 32.73142 | 123.6504 | 26.861 | 27.13727 | 0.276268 |
| 36.2579 | 123.2191 | 24.745 | 24.00082 | -0.744176 |
| 36.65023 | 122.782 | 24.282 | 23.75211 | -0.529894 |

## IV. PERFORMANCE TEST

### A. LAKE SUSPENDED SEDIMENT CONCENTRATION TEST ENVIRONMENT

The data of this research comes from the Noaa-19AVHRR/3 shooting data between 4 am and 6 am provided by the website of the National Oceanic and Atmospheric Administration of the United States. The orbit of the Noaa-19 satellite is a sun-synchronous orbit close to a perfect circle, with orbital heights of 870 kilometers and 833 kilometers, orbital inclination angles of 98.9 and 98.7, and a period of 101.4 minutes. AVHRR/3 parameters include 5 bands, visible red band, near-infrared band, mid-infrared band and two thermal infrared bands.

### B. SIMULATION OF SUSPENDED SEDIMENT CONCENTRATION IN LAKE

In order to achieve the inversion of suspended sediment concentration satellite data, we introduced ADAM and deep learning algorithms in the process. Through the satellite data inversion model of lake suspended sediment concentration

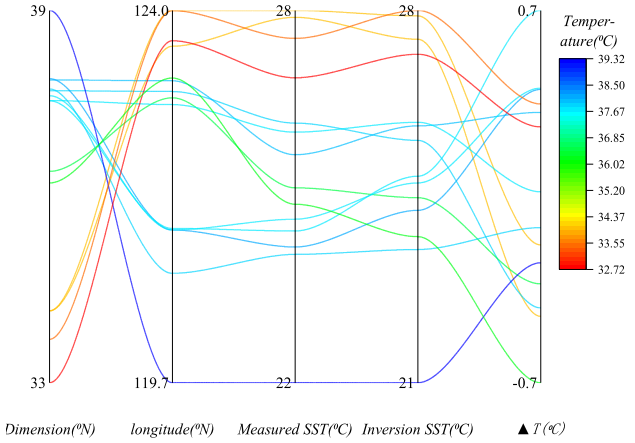


**FIGURE 3.** Change trend of sea surface temperature data from satellite remote sensing.

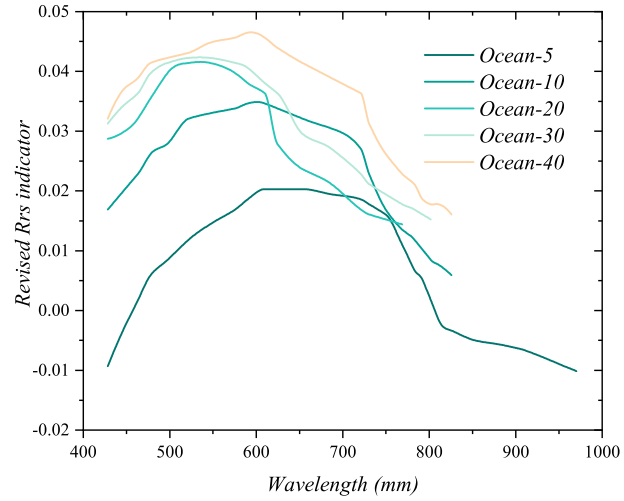


**FIGURE 4.** Satellite data inversion of off-water reflectivity-offshore area.

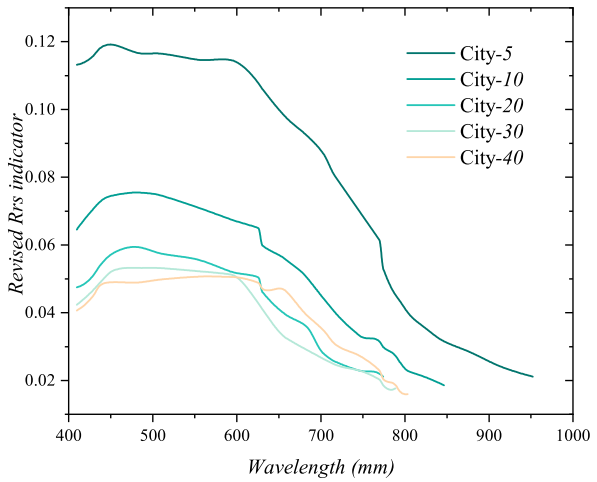


**FIGURE 5.** Satellite data inversion of out-of-water reflectivity-urban area.

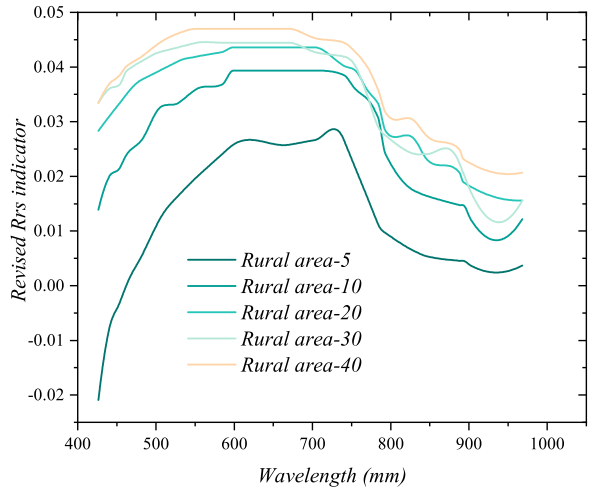


**FIGURE 6.** Satellite data inversion of out-of-water reflectivity-rural areas.

established in the third chapter, we will carry out the sediment concentration simulation test process.

By correcting the satellite remote sensing data, the out-of-water reflectance Rrs of each pixel can be obtained. Different atmospheric correction schemes will have different atmospheric correction parameters and therefore different Rrs result values. Fig. 4, Fig. 5, Fig. 6 and Fig. 7 respectively show the out-of-water reflectance Rrs under the same atmospheric correction scheme (a combination of 4 aerosol types and 5 visibility). The 3 points selected here are from the high turbidity zone, the moderate turbidity zone and the low turbidity zone. In these four figures, the ocean, rural area, city, and plateau represent different aerosol types. 5, 10, 20, 30 and 40 respectively represent visibility, and the unit is km. The reflectance from water Rrs is not only a function of wavelength but also a function of atmospheric conditions.

Compared with the other two aerosols, the Rrs value from the urban aerosol correction scheme has a larger range of variation. Using the urban aerosol scheme, all the correction results are positive, which is in line with the facts, and the maximum value reaches 0.12, which rarely occurs in reality. When the visibility is 5 km, the correction result of the ocean and rural aerosol scheme is negative, which is considered wrong, because the value of the reflectance from the water is between 0-1, so the actual visibility must be 5 at that time. km above. It can be seen from the figure that the visibility range from 5 km to 20 km, Rrs is very different, so in this visibility range, Rrs is very sensitive to visibility, which explains that the previous chapter mentioned that the distance between 5km and 5km is very sensitive. 2 km is the reason for linear difference to improve accuracy. However, from 20 km to 40 km, since Rrs is not so sensitive to visibility, this paper keeps the original setting of 10 km increments.

By setting a series of SSC values, the corresponding Rrs value can be simulated. Because the research focus of this article is suspended sediment. In order to simplify the model, the average concentration of chlorophyll and yellow substances is used in this article. For chlorophyll, 3 different average concentration values are used for different regions. For yellow substances, this article only takes an average value for the entire research field. Figures 8 and 9 show the simulated results. The value of SSC is from $10^0$ to $10^{3.5}$ mg/1, and

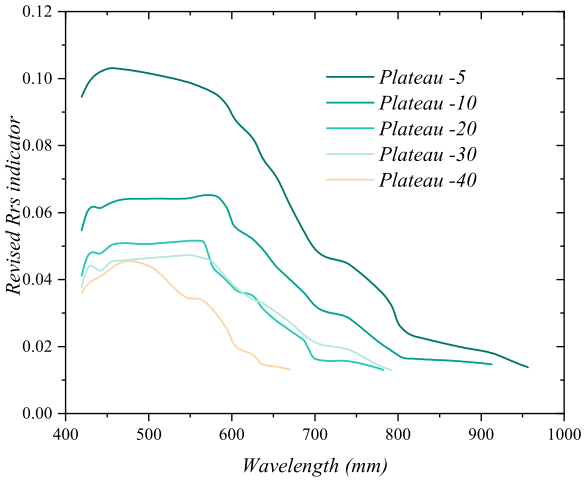


**FIGURE 7.** Satellite data inversion of out-of-water reflectivity-plateau area.

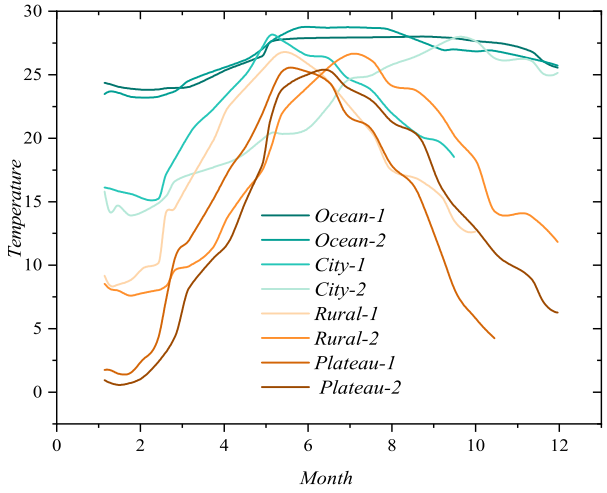


**FIGURE 8.** Seasonal changes in temperature simulated by inversion of satellite data.

the index increases by 0.002 each time. Figure 9 shows the value of every 50 increments. The concentration of chlorophyll is 2mg/m$^3$, and the concentration of yellow substance is 0.215 mg/m$^3$.

In Figure 9, it is obvious that there are two peaks. The first peak is wider than the second peak. The first peak is approximately from 590 nm to 730 nm. In the short-wave visible light band, the reflectivity from water is very low, because of the strong absorption of chlorophyll and other substances in the water body at this band. As the wavelength increases, the scattering energy of suspended sand until Rrs reaches the first peak. We introduced ADAM and deep learning algorithms in this process. Through the above simulation process, it can be concluded that the model established in this paper has solved the work of inversion of suspended sediment concentration data. The second peak of the wavelength increase is around 820 nm, and the reflection increases. Water color remote sensing is based on the spectral characteristics of water absorption and scattering in visible light or

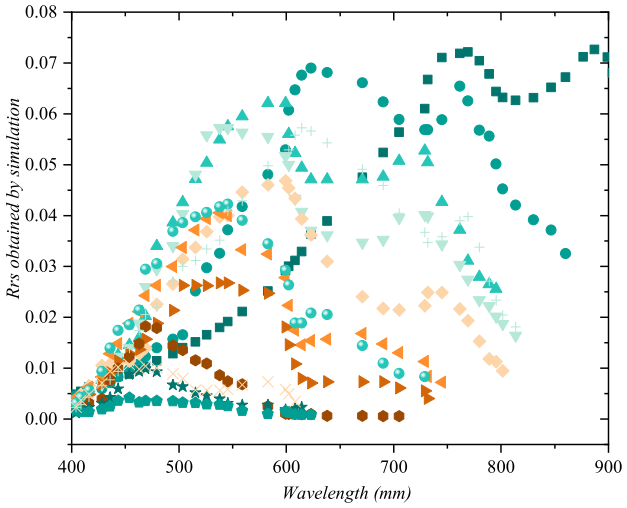


**FIGURE 9.** The simulated changes of Rrs with wavelength under different suspended sediment concentration.

near-infrared, using the water-separated spectrum radiation data measured by aviation and aerospace sensors to interpret the relevant phenomena and parameters of the water body. With the help of remote sensing technology, the information on the concentration of suspended sediment that traditional methods require a lot of work can be obtained faster, better, and more easily. When the concentration of suspended sediment increases, the force continues to increase, and the peak shifts to the right. The two peaks are similar in size. The second peak is more stable than the first peak, and its position is at the low absorption band of the spectral radiation of water molecules.

## V. CONCLUSION

The distribution pattern of suspended sediment is of great significance to the study of water quality, geomorphology, ecological environment, coastal engineering, and port construction. With the help of remote sensing technology, the information on the concentration of suspended sediment that traditional methods require a lot of work can be obtained faster, better, and more easily. Water color remote sensing is based on the spectral characteristics of water absorption and scattering in visible light or near-infrared, using the water-separated spectrum radiation data measured by aviation and aerospace sensors to interpret the relevant phenomena and parameters of the water body. The main purpose of this thesis is to use the concentration of suspended sediment as the research object to explore the method of remote sensing to monitor the water quality of large lakes. This paper combines the results of satellite remote sensing inversion and the results of on-site water sample inspections of the Internet of Things to obtain the original hydrological data of suspended sediment in lakes. This paper combines ADAM and deep learning technology to simulate the lake flow field to predict the dynamic process of suspended sediment pollution under different conditions. We have verified the effectiveness of the lake suspended sediment concentration model established in

this paper through experimental simulation and field sampling tests. Although this paper successfully established a temporal and spatial distribution model of suspended sediment concentration in lakes based on the Internet of Things, due to the limitations of personal knowledge, we still have certain deficiencies in experimental accuracy and the design of the Internet of Things structure. In the future, we will continue to maintain a cautious and forward attitude and devote ourselves to providing a research reference and reference for the modern lake environment and sustainable development. In future research, how to use the latest remote sensing images to predict lake changes is the main research direction. This can improve the prediction of the impact of lake changes on the surrounding environment and predict future changes.

## REFERENCES

[1] H. Zhu, S. Lee, H.-B. Moon, and K. Kannan, "Spatial and temporal trends of melamine and its derivatives in sediment from Lake Shihwa, South Korea," *J. Hazardous Mater.*, vol. 373, pp. 671–677, Jul. 2019.

[2] C. Zhan, C. Dong, T. Wang, B. Li, Y. Liu, and X. Yu, "Remotely sensed retrieval of extreme high surface suspended sediment concentration in the yellow river estuary from 1996 to 2017," *J. Coastal Res.*, vol. 99, no. 1, p. 221, May 2020.

[3] J. Ying, K. Liang, Q. Wu, M. Xie, X. Jin, Q. Ye, and Z. Yang, "Calculation of suspended sediment concentration based on deep learning and OBS turbidity," *J. Coastal Res.*, vol. 115, no. 1, p. 627, Aug. 2020.

[4] K. Xu, Q. Tian, Y. Yang, J. Yue, and S. Tang, "How up-scaling of remote-sensing images affects land-cover classification by comparison with multi-scale satellite images," *Int. J. Remote Sens.*, vol. 40, no. 7, pp. 2784–2810, Apr. 2019.

[5] J. Wei, X. Yu, Z. Lee, M. Wang, and L. Jiang, "Improving low-quality satellite remote sensing reflectance at blue bands over coastal and inland waters," *Remote Sens. Environ.*, vol. 250, Dec. 2020, Art. no. 112029.

[6] L. L. Thurston, E. Schiefer, N. P. McKay, and D. S. Kaufman, "Modelling suspended sediment discharge in a glaciated Arctic catchment-Lake Peters, northeast Brooks Range, Alaska," *Hydrol. Processes*, vol. 34, no. 19, pp. 3910–3927, Sep. 2020.

[7] M. J. Sayers, G. L. Fahnenstiel, R. A. Shuchman, and K. R. Bosse, "A new method to estimate global freshwater phytoplankton carbon fixation using satellite remote sensing: Initial results," *Int. J. Remote Sens.*, vol. 42, no. 10, pp. 3708–3730, May 2021.

[8] M. River and C. J. Richardson, "Suspended sediment mineralogy and the nature of suspended sediment particles in stormflow of the Southern Piedmont of the USA," *Water Resour. Res.*, vol. 55, no. 7, pp. 5665–5678, Jul. 2019.

[9] Q. Qi, X. Chen, C. Zhong, and Z. Zhang, "Integration of energy, computation and communication in 6G cellular Internet of Things," *IEEE Commun. Lett.*, vol. 24, no. 6, pp. 1333–1337, Jun. 2020.

[10] P. Gong, X. Li, and W. Zhang, "40-year (1978–2017) human settlement changes in China reflected by impervious surfaces from satellite remote sensing," *Sci. Bull.*, vol. 64, no. 11, pp. 756–763, Jun. 2019.

[11] C. B. Obida, G. A. Blackburn, J. D. Whyatt, and K. T. Semple, "Counting the cost of the Niger Delta's largest oil spills: Satellite remote sensing reveals extensive environmental damage with >1million people in the impact zone," *Sci. Total Environ.*, vol. 775, Jun. 2021, Art. no. 145854.

[12] M. Nazeer, C. O. Ilori, M. Bilal, J. E. Nichol, W. Wu, Z. Qiu, and B. K. Gayene, "Evaluation of atmospheric correction methods for low to high resolutions satellite remote sensing data," *Atmos. Res.*, vol. 249, Feb. 2021, Art. no. 105308.

[13] S. Miyata, S. Mizugaki, S. Naito, and M. Fujita, "Application of time domain reflectometry to high suspended sediment concentration measurements: Laboratory validation and preliminary field observations in a steep mountain stream," *J. Hydrol.*, vol. 585, Jun. 2020, Art. no. 124747.

[14] A. Mitra and V. S. Kumar, "A numerical investigation on the tide-induced residence time and its association with the suspended sediment concentration in Gulf of Khambhat, northern Arabian Sea," *Mar. Pollut. Bull.*, vol. 163, no. 12, Feb. 2021, Art. no. 111947.

[15] S. N. Matheu, J. L. Hernández-Ramos, A. F. Skarmeta, and G. Baldini, "A survey of cybersecurity certification for the Internet of Things," *ACM Comput. Surv.*, vol. 53, no. 6, pp. 1–36, Feb. 2021.

[16] A. Manocha, R. Singh, and P. Verma, "An Internet of Things fog-assisted sleep-deprivation prediction framework for spinal cord injury patients," *Computer*, vol. 53, no. 2, pp. 46–56, Feb. 2020.

[17] W. Liu, T. Peng, R. Tang, Y. Umeda, and L. Hu, "An Internet of Things-enabled model-based approach to improving the energy efficiency of aluminum die casting processes," *Energy*, vol. 202, Jul. 2020, Art. no. 117716.

[18] G. Lim, R. Jayaratne, and T. Shibayama, "Suspended sand concentration models under breaking waves: Evaluation of new and existing formulations," *Mar. Geol.*, vol. 426, Aug. 2020, Art. no. 106197.

[19] Y. Li, L. Xie, and T. C. Su, "Profile of suspended sediment concentration in submerged vegetated shallow water flow," *Water Resour. Res.*, vol. 56, no. 4, Apr. 2020, Art. no. e2019WR025551.

[20] D. Li, Z. Yang, Z. Zhu, M. Guo, W. Gao, and Z. Sun, "Estimating the distribution of suspended sediment concentration in submerged vegetation flow based on gravitational theory," *J. Hydrol.*, vol. 587, Aug. 2020, Art. no. 124921.

[21] C. K. F. Lee, E. Nicholson, C. Duncan, and N. J. Murray, "Estimating changes and trends in ecosystem extent with dense time-series satellite remote sensing," *Conservation Biol.*, vol. 35, no. 1, pp. 325–335, Feb. 2021.

[22] J. T. Kemper, A. J. Miller, and C. Welty, "Spatial and temporal patterns of suspended sediment transport in nested urban watersheds," *Geomorphology*, vol. 336, pp. 95–106, Jul. 2019.

[23] K. Fawaz and K. G. Shin, "Security and privacy in the Internet of Things," *Computer*, vol. 52, no. 4, pp. 40–49, Apr. 2019.

[24] L. Fichera, G. Li-Destri, and N. Tuccitto, "Fluorescent nanoparticle-based Internet of Things," *Nanoscale*, vol. 12, no. 17, pp. 9817–9823, 2020.

[25] N. J. C. Doriean, P. R. Teasdale, D. T. Welsh, A. P. Brooks, and W. W. Bennett, "Evaluation of a simple, inexpensive, *in situ* sampler for measuring time-weighted average concentrations of suspended sediment in rivers and streams," *Hydrol. Processes*, vol. 33, no. 5, pp. 678–686, Feb. 2019.

[26] S. Debnath, K. Ghoshal, and J. Kumar, "Unsteady two-dimensional suspended sediment transport in open channel flow subject to deposition and re-entrainment," *J. Eng. Math.*, vol. 126, no. 1, pp. 1–13, Feb. 2021.

[27] Y. Chen, R. M. Hozalski, L. G. Olmanson, B. P. Page, J. C. Finlay, P. L. Brezonik, and W. A. Arnold, "Prediction of photochemically produced reactive intermediates in surface waters via satellite remote sensing," *Environ. Sci. Technol.*, vol. 54, no. 11, pp. 6671–6681, Jun. 2020.

[28] W.-C. Chen, J.-S. Niu, I.-P. Liu, C.-Y. Chi, S.-Y. Cheng, K.-W. Lin, and W.-C. Liu, "Study of a palladium (Pd)/aluminum-doped zinc oxide (AZO) hydrogen sensor and the Kalman algorithm for Internet-of-Things (IoT) application," *IEEE Trans. Electron Devices*, vol. 67, no. 10, pp. 4405–4412, Oct. 2020.

[29] J. Chauhan and P. Goswami, "An integrated metaheuristic technique based energy aware clustering protocol for Internet of Things based smart classroom," *Mod. Phys. Lett. B*, vol. 34, no. 22, Aug. 2020, Art. no. 2050360.

[30] W. Zhan, J. Wu, X. Wei, S. Tang, and H. Zhan, "Spatio-temporal variation of the suspended sediment concentration in the Pearl River Estuary observed by MODIS during 2003–2015," *Continental Shelf Res.*, vol. 172, pp. 22–32, Jan. 2019.

[31] L. P. Bitencourt, E. H. Fernandes, P. D. D. Silva, and O. Möller, "Spatio-temporal variability of suspended sediment concentrations in a shallow and turbid lagoon," *J. Mar. Syst.*, vol. 212, Dec. 2020, Art. no. 103454.

[32] A. Villa-Henriksen, G. T. C. Edwards, L. A. Pesonen, O. Green, and C. A. G. Sørensen, "Internet of Things in arable farming: Implementation, applications, challenges and potential," *Biosyst. Eng.*, vol. 191, pp. 60–84, Mar. 2020.

[33] H. Arfaeinia, S. Dobaradaran, M. Moradi, H. Pasalari, E. A. Mehrizi, F. Taghizadeh, A. Esmaili, and M. Ansarizadeh, "The effect of land use configurations on concentration, spatial distribution, and ecological risk of heavy metals in coastal sediments of northern part along the Persian Gulf," *Sci. Total Environ.*, vol. 653, pp. 783–791, Feb. 2019.

[34] S. M. Amini and A. Karimi, "Two-level distributed clustering routing algorithm based on unequal clusters for large-scale Internet of Things networks," *J. Supercomput.*, vol. 76, no. 3, pp. 2158–2190, Mar. 2020.

[35] R. Abbasi-Kesbi, A. Nikfarjam, and M. Nemati, "Developed wireless sensor network to supervise the essential parameters in greenhouses for Internet of Things applications," *IET Circuits, Devices Syst.*, vol. 14, no. 8, pp. 1258–1264, Nov. 2020.